

## Actin Can Reorganize into Podosomes in Aortic Endothelial Cells, a Process Controlled by Cdc42 and RhoA

Violaine Moreau,\* Florence Tatin, Christine Varon, and Elisabeth Génot

*Institut Européen de Chimie-Biologie, INSERM U441, 33600 Pessac, France*

Received 15 January 2003/Returned for modification 26 February 2003/Accepted 24 June 2003

**Members of the Rho GTPase family play a central role in the orchestration of cytoskeletal rearrangements, which are of prime importance in endothelial cell physiology. To explore their role in this specialized cell type, we used the bacterial toxin cytotoxic necrotizing factor 1 (CNF1) as a Rho GTPase activator. Punctate filamentous actin structures appeared along the ventral plasma membrane of endothelial cells and were identified as the core of podosomes by the distinctive vinculin ring around the F-actin. Rho, Rac, and Cdc42 were all identified as targets of CNF1, but only a constitutively active mutant of Cdc42 could substitute for CNF1 in podosome induction. Accordingly, organization of F-actin in these structures was highly dependent on the main Cdc42 cytoskeletal effector N-Wiskott-Aldrich syndrome protein. Other components of the actin machinery such as Arp2/3 and for the first time WIP also colocalized at these sites. Like CNF1 treatment, sustained Cdc42 activity induced a time-dependent F-actin–vinculin reorganization, prevented cytokinesis, and downregulated Rho activity. Finally, podosomes were also detected on endothelial cells explanted from patients undergoing cardiac surgery. These data provide the first description of podosomes in endothelial cells. The identification of such specialized structures opens up a new field of investigation in terms of endothelium pathophysiology.**

Actin cytoskeleton rearrangements are the basis of many fundamental processes of cell biology such as motility, adhesion, mitosis, endocytosis, and morphogenesis. In various models, the cytoskeletal dynamics underlying these processes have been shown to be driven by small G-protein members of the Rho family, a subclass of the Ras superfamily. Like most of these small GTP-binding proteins, Rho GTPases cycle between an inactive GDP-bound and an active GTP-bound form. In this state, GTPases are able to interact with and thereby activate downstream targets, the so-called effectors. Guanine exchange factors catalyze the exchange of GDP for GTP and hence activate the GTPases, whereas the GTPase-activating proteins enhance the intrinsic GTPase activity, returning the GTPases to their basal GDP-bound state (52). Alternatively, specific alterations of the GTPase, such as covalent modifications by bacterial toxins or point mutations on key residues, prevent nucleotide exchange or GTP hydrolysis, thereby locking the GTPase into one conformation or the other. In the last few years, toxins and GTPase mutants have turned out to be valuable tools for deciphering the signaling networks and characterizing downstream pathways of this class of GTPases, of which Rho, Rac, and Cdc42 are the best-characterized members.

Activation of Rho GTPases can be achieved in two different ways: by soluble factors binding to cell surface receptors or by extracellular matrix components interacting with clustered adhesion molecules of the integrin family. The Rho GTPases regulate actin dynamics by acting as molecular switches that transduce signals from activated membrane receptors to cy-

toskeleton organizers (52). When microinjected into fibroblasts, constitutively activated mutants of RhoA generate actin stress fibers and those of Rac1 induce lamellipodia, whereas constitutive active Cdc42 stimulates the formation of microspikes or filopodia (37). Cdc42 interacts with a variety of targets such as Wiskott-Aldrich syndrome protein (WASP), the protein kinases from the PAK (p21-activated kinase) family, and ACK (activated Cdc42-associated tyrosine kinase) (12), thereby influencing a diverse range of cellular responses including cell growth, RNA processing, and intracellular vesicle traffic both at the level of receptor-mediated endocytosis and transport from the Golgi stacks (12).

In addition to stress fibers, lamellipodia, and filopodia, actin can also be arranged into peculiar dot-like structures called podosomes, because they were first thought to represent cellular feet (51). Ultrastructural analysis by transmission electron microscopy showed that podosomes are in fact peculiar glove finger invaginations found at the ventral membrane of the cell and directed towards the center, perpendicularly from the substratum (36). Podosomes share major structural components with focal contacts but are distinct in size, morphology, organization, and turnover. They are composed of a core of actin filaments and actin-associated proteins, surrounded by a ring of vinculin, talin, and paxillin (17). Such actin-based attachment structures are constitutively found in monocyte-derived hematopoietic cells including osteoclasts, macrophages, leukocytes, and immature dendritic cells, where they are believed to play a role in bone resorption, migration, diapedesis, and motility, respectively. In pathological settings, podosome formation has been observed in fibroblasts transformed by the Rous sarcoma virus (51). Recent data suggest that podosomes play a role in extracellular matrix degradation (32) similar to that of invadopodia, a related protrusive structure (7). Thus, podosomes appear to be structures that com-

\* Corresponding author. Mailing address: INSERM U441, Institut Européen de Chimie-Biologie, Avenue du Haut-Lévêque, 33600 Pessac, France. Phone: 33 5 57890101. Fax: 33 5 56368979. E-mail: v.moreau@iecb-polytechnique.u-bordeaux.fr.

bine adhesive functions with proteolytic degradation of the extracellular matrix.

Little is known about podosome formation. Distinct molecular pathways have been described depending on the cell type considered, but Rho GTPases are always involved. In osteoclasts, podosome formation is dependent on Rho activity (6, 58). In macrophages, Cdc42 localizes at podosomes but its activation disrupts podosome organization (28). More recently, podosome assembly and polarization have been shown to require the concerted action of Cdc42, Rac, and Rho in immature dendritic cells (4). Finally, the Cdc42 effector WASP has been involved in podosome formation in primary human macrophages, in immature dendritic cells, and in rat 3Y1 fibroblasts transformed with *v-src* (4, 28, 32), suggesting that Cdc42 could be a common upstream regulator of podosome assembly in distinct cell types.

The endothelial cell cytoskeleton is particularly exposed to remodeling. Cytoskeletal dynamics is of prime importance in the physiology of endothelial cells engaged in an angiogenic or vasculogenic program. In the endothelium, cytoskeletal organization is regulated by adhesive interactions with neighboring cells or the extracellular matrix and allows endothelial permeability and vessel wall integrity. Plasticity is required for correct extravasation of blood-borne leukocytes at sites of inflammation. Lastly, the endothelial cells lining blood vessels are constantly subjected to shear stress, the tangential component of hemodynamic forces caused by blood flow, and this significantly influences their phenotype. In the present study, we have analyzed actin rearrangements in relation with GTPase activity in endothelial cells.

## MATERIALS AND METHODS

**Culture conditions and cell intoxication.** Porcine aortic endothelial (PAE) cells (clone p23) (18) were maintained in F-12 medium (Ham F-12; GIBCO BRL) supplemented with 10% heat-inactivated fetal calf serum (FCS) at 37°C in a 5% CO<sub>2</sub> humidified atmosphere. PAE cell lines expressing either V12, N17, or wild-type (wt) Cdc42 under the control of an isopropyl- $\beta$ -D-thiogalactopyranoside (IPTG)-inducible promoter were established previously (8) and cultured in the same medium supplemented with 100  $\mu$ M hygromycin B and 500 nM puromycin. Expression was achieved by 0.1 mM IPTG. For *Escherichia* cytotoxic necrotizing factor 1 (CNF1) intoxication, cells were treated with 500 ng of glutathione *S*-transferase (GST)-CNF1 per ml 1 day after seeding. For *Clostridium botulinum* C3 exoenzyme intoxication, PAE V12Cdc42 cells were treated with 5  $\mu$ g of Tat-C3 per ml for 24 h.

**Cells transfection.** Cells were transfected by using TransFast reagent (Promega Corporation) according to the manufacturer's instructions. Briefly, cells were seeded on coverslips at 50 to 70% confluence 1 day before transfection. For each coverslip, 0.5  $\mu$ g of DNA, 1.5  $\mu$ l of TransFast reagent, and 200  $\mu$ l of serum-free medium were mixed and incubated on cells for 1 h. Complete medium was added, and cells were fixed and processed for immunofluorescence 24 h after transfection.

**Reagents and antibodies.** Puromycin, hygromycin B, IPTG, and Mowiol 4-88 were from Calbiochem. FCS was from Globepharm, and culture medium and antibiotics were from Gibco. Glutathione-Sepharose beads, propidium iodide, dimethyl sulfoxide, lipophosphatidic acid (LPA), bacterial collagenase type IV, fibronectin, and various chemicals were from Sigma. CNF1 and TatC3 were kindly supplied by J. Bertoglio (INSERM U461, Chatenay-Malabry, France). Rhodamine-phalloidin and fluorescein isothiocyanate-labeled secondary antibodies were purchased from Molecular Probes. Monoclonal antivinculin (hVIN-1) and antiVon-Willebrand factor were from Sigma, and anti-myc (9E10) and anti-phosphotyrosine (4G10) were kind gifts from Doreen Cantrell (London, United Kingdom). Anti-gelsolin antibody was kindly supplied by C. Chaponnier (University of Geneva, Geneva, Switzerland). Polyclonal Arp3 antibody was a generous gift from M. Welch (University of California, Berkeley). Anti-Rho,

-Rac, and -Cdc42 antibodies were purchased from Upstate Biotechnology and Transduction Laboratories.

**Expression constructs.** Plasmids encoding GST-Rho-binding domain (RBD)-rhotekin and GST-Cdc42/Rac-interactive binding domain (CRIB)-PAK have been described elsewhere (43, 45). Constructs encoding wt, active, or dominant-negative mutants of either green fluorescent protein (GFP)-Rho, -Rac, or -Cdc42 were made and kindly provided by P. Fort (CNRS-UPR1086, Montpellier, France). The GFP expression vectors for N-WASP were previously reported (33). The GFP-WIP and GFP-WASP-interacting protein (WIP)-WASP binding domain constructs were subcloned from pEL vectors (33) into the eucaryotic pCB6 vectors.

**Immunofluorescence microscopy.** Subconfluent cells grown on glass coverslips were fixed with 3% paraformaldehyde prepared in cytoskeletal buffer (CB) (10 mM morpholineethanesulfonic acid, 150 mM NaCl, 5 mM EGTA, 5 mM MgCl<sub>2</sub>, and 5 mM glucose [pH 6.1]) for 10 min at room temperature and permeabilized with 0.1% Triton X-100 for 1 min. After 3 washes in CB, the cells were incubated in blocking solution (1% bovine serum albumin, 2% FCS in Tris-buffered saline) for 10 min, in primary antibody diluted in blocking solution for 30 min, and then in fluorescently labeled secondary antibody for 30 min. Between each step, cells were washed 3 times with Tris-buffered saline (20 mM Tris, 150 mM NaCl, 2 mM EGTA, 2 mM MgCl<sub>2</sub> [pH 7.5]). The coverslips were washed in water and mounted on microscope slides with Mowiol 4-88 mounting medium. Cells were analyzed by confocal microscopy with an Eclipse E800 Nikon microscope. The images were processed with Adobe Photoshop 5.5. Quantitation of cells showing podosomes was assessed in three independent experiments in which at least 200 cells were counted.

**Rho, Rac, and Cdc42 activity assays.** The Rho, Rac, and Cdc42 activity assays are based on the Rap1 activity assay (15). Rho protein activity assays were performed essentially as described in published protocols (41, 44).

**Preparation of endothelial cells from aortic explants.** Endothelial cells were isolated from freshly explanted human aorta fragments from patients undergoing cardiac surgery by using a modified version of a published protocol (3). The vessel was cut off under sterile conditions and cleaned free of connective tissue. The adventitia was peeled off from the media, and the fragment was incubated with collagenase. Endothelial cells were then harvested from the subendothelial bed and seeded on a glass coverslip in culture medium. The attached cells were then fixed, permeabilized, and processed for immunofluorescence. After 24 h, endothelial cells (80 to 85% cells positive for Von-Willebrand factor) formed round colonies of 5 to 30 cells.

## RESULTS

**CNF1 induces podosome-like structure formation in PAE cells.** To explore the role of Rho GTPases in endothelial cells, we used the bacterial toxin CNF1 as a general in vitro activator of Rho GTPases. CNF1 induces activation of Rho, Rac, and Cdc42 through the deamidation of a pivotal glutamine residue (Gln63 for Rho and Gln61 for Rac and Cdc42) essential for GTP hydrolysis (14, 25, 47). By inhibiting both intrinsic and glyceraldehyde-3-phosphate (GAP)-catalyzed GTPase activity, this alteration renders the protein constitutively active. As for epithelial cells (13, 25), treatment of endothelial cells with CNF1 (fused to GST [GST-CNF1]) induced dramatic morphological changes. With time, cells progressively increased in size and became multinucleated (data not shown). To visualize the actin cytoskeleton, polymerized actin was stained with rhodamine-labeled phalloidin. F-actin staining revealed a profound reorganization of the cytoskeleton (Fig. 1A). In contrast to epithelial cell types, neither lamellipodia, filopodia, nor microspikes were detected, but membrane ruffling and classical stress fibers remained visible. The most striking change observed under toxin treatment was the formation of dot-like structures uniformly dispatched throughout the cell body (Fig. 1A). These structures appeared after 2 h of GST-CNF1 treatment and remained in cells for up to several days. With time, the number of actin dots per cell increased along with cell size and the percentage of positive cells (25% at 24 h and 42% at

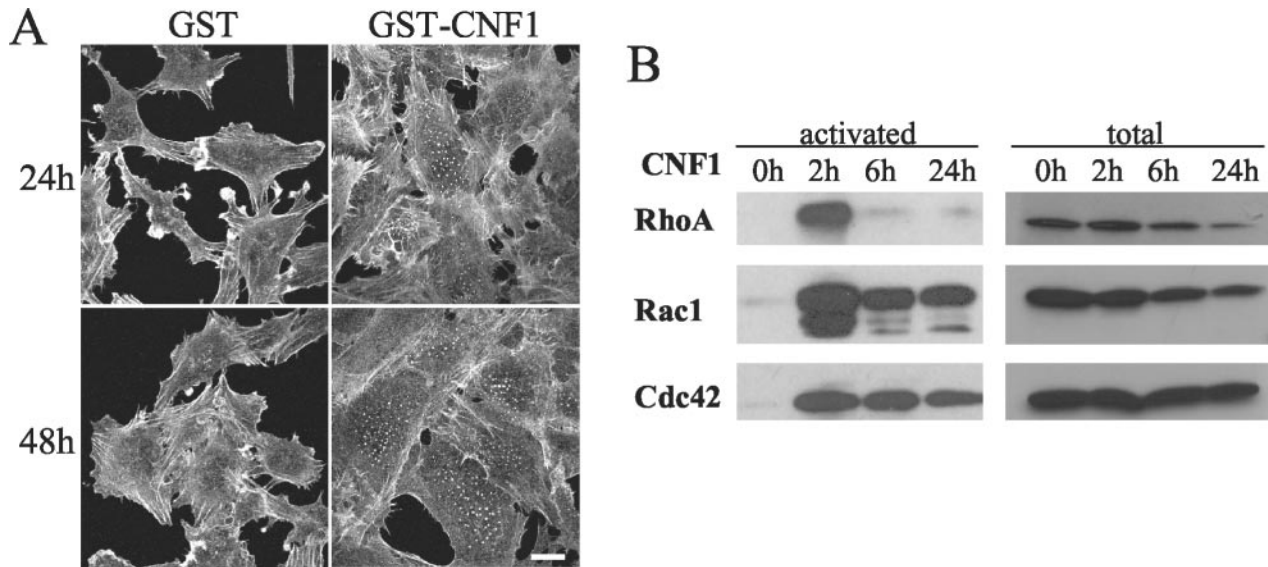


FIG. 1. Effects of CNF1 on PAE cells. (A) PAE cells were treated with 0.5  $\mu$ g of GST alone or GST-CNF1 per ml for 24 or 48 h. Cells were then fixed, permeabilized, and stained with rhodamine-phalloidin. Bar, 50  $\mu$ m. (B) CNF1 activates RhoA, Rac1, and Cdc42 in PAE cells. Cells were treated with 0.5  $\mu$ g of GST-CNF1/ml for 0, 2, 6, and 24 h. Cells were then lysed, and active GTPases were affinity precipitated with GST-RBD-rhotekin or GST-CRIB-PAK, eluted from the beads, and analyzed by Western blotting with the relevant antibodies. For each point, a fraction of the lysate was run to monitor the amount of GTPase before precipitation.

48 h). No similar reorganization of the actin cytoskeleton was detected upon addition of GST alone (Fig. 1A).

**CNF1 activates Rho, Rac, and Cdc42 in PAE cells.** We next aimed to determine which members of the Rho family of GTPases are activated by CNF1 in PAE cells by using the pull-down method. GST fusion proteins containing GTPase binding domains of effectors, rhotekin for Rho (41) and the CRIB of PAK for Rac and Cdc42 (44), were coupled to agarose beads to precipitate GTP-bound GTPases from CNF1-treated or control PAE cells. Then, affinity-purified proteins were analyzed by electrophoresis followed by Western blotting with GTPase-specific antibodies. RhoA was rapidly activated upon CNF1 treatment, but this activation was only transient, with a peak at 2 h and undetectable levels after 6 h (Fig. 1B). Compared to Rho, activation of Rac1 and Cdc42 was equally rapid but more sustained and still fully detectable after 24 h. Prolonged exposure to CNF1 caused the disappearance of the three GTPases, with a more acute effect on Rho. This effect could result from proteolytic degradation of the CNF1-modified GTPases by a proteasome-dependent pathway (10). From these experiments, we concluded that CNF1 treatment affects Rho, Rac, and Cdc42 GTPases in PAE cells.

**Activation of Cdc42 causes the formation of dot-like structures and loss of stress fibers.** Although the three Rho GTPases were found to be activated by CNF1, we anticipated that not all three GTPases would be required for the observed dot-like structure assembly. To assess the individual role of each GTPase in this process, PAE cells were transfected with plasmids encoding GFP-tagged activated mutants of either Rho, Rac, or Cdc42. Cells expressing recombinant proteins were identified by GFP fluorescence 24 h after transfection, and their actin cytoskeletons were examined by rhodamine-phalloidin staining. As expected (37), the constitutively activated forms of RhoA and Rac1 induced stress fiber and lamel-

lipodia formation, respectively (Fig. 2A). However, GFP-V12Cdc42 induced cells to lose stress fibers and to form dot-like structures (Fig. 2A), a phenotype reminiscent of that observed in CNF1-treated cells (Fig. 1A). Moreover, GFP-Cdc42 localized to the dot-like structures positive for actin (Fig. 2A) and to the Golgi region as previously shown (31). Nevertheless, control experiments showed that this GFP fusion protein was able to induce filopodia in NIH 3T3 fibroblasts (Fig. 2A).

To confirm the role of Cdc42 in the formation of dot-like structures, we made use of three established PAE cell lines in which overexpression of Cdc42 (wtCdc42) or of its mutated forms (constitutively active V12Cdc42 or dominant-negative N17Cdc42) is under the control of an IPTG-inducible promoter (8). V12Cdc42-expressing PAE cells rearranged their actin cytoskeletons in a way that was indistinguishable from cells transiently transfected with GFP-V12Cdc42 (Fig. 2B). By contrast, the dot-like structures remained absent from the IPTG-induced N17Cdc42 or wtCdc42 cell lines (data not shown). Punctate staining was noted in a few cells 4 h after IPTG induction and coincided with V12Cdc42 protein detection in Western blotting experiments (data not shown). At 24 h, about 55% of the cells had increased in volume, flattened, and lost their stress fibers. The number of cells presenting isolated or scattered dots had increased to 43%. By 48 h, all cells were enlarged and the actin cytoskeleton of most of them had reorganized into actin dots. Filopodia-like protrusions could also be observed at the periphery of V12Cdc42-expressing PAE cells. Concomitant with the occurrence of this new actin configuration and morphological changes, the cells became multinucleated (Fig. 2B). Cells counts showed that proliferation had not occurred throughout the IPTG induction process (data not shown), strongly suggesting that cytokinesis was impaired. Finally, removal of IPTG caused disassembly of

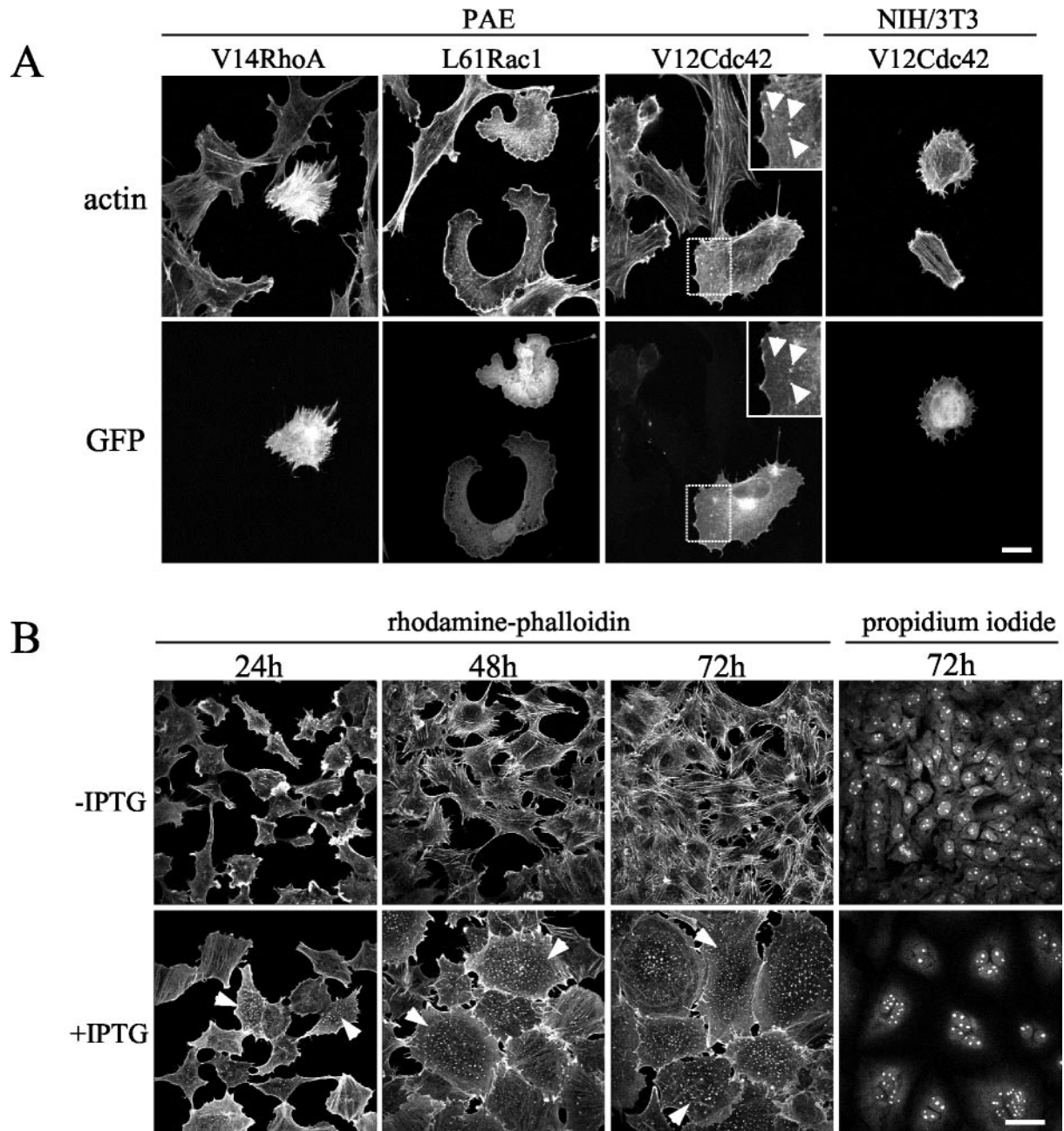


FIG. 2. Activated form of Cdc42 leads to actin-dot formation. (A) PAE cells were transfected with GFP-V14RhoA, GFP-L61Rac1, or GFP-V12Cdc42. NIH 3T3 cells were transfected with GFP-V12Cdc42. Twenty-four hours later, cells were fixed and processed for immunofluorescence. F-actin was labeled with rhodamine-phalloidin, and cells expressing the GFP-tagged constructs were visualized by the green GFP signal. Dot-like structures are shown (arrowheads). Bar, 50  $\mu$ m. (B) Established PAE cells in which expression of V12Cdc42 is under the control of an IPTG-inducible promoter were induced with (+IPTG) or without (-IPTG) IPTG. Cells were fixed after 24, 48, and 72 h. F-actin was labeled with rhodamine-phalloidin, and nuclei were labeled with propidium iodide. Cells displaying dot-like structures are shown (arrowheads). Bar, 100  $\mu$ m.

the dot-like structures and complete reversion of the phenotype. Taken together, these results establish that morphological alterations, dot-shaped actin-configuration acquisition, and defects in cytokinesis are common features of CNF1-treated and V12Cdc42-expressing PAE cells.

**The dot-like structures are podosomes.** Podosomes represent an uncommon type of actin organization, only found so far in restricted subsets of cells from the hematopoietic lineage

and dedicated to specific functions all involving adhesion. Therefore, in the context of endothelial cells, it was relevant to establish whether these dot-like structures represented real podosomes. A stack of optical sections obtained by confocal microscopy showed that actin dots were exclusively found at the ventral surface of the endothelial cell (Fig. 3). The original protocol described by Tarone et al. to evidence the adhesive nature of podosomes was used to investigate the interaction of

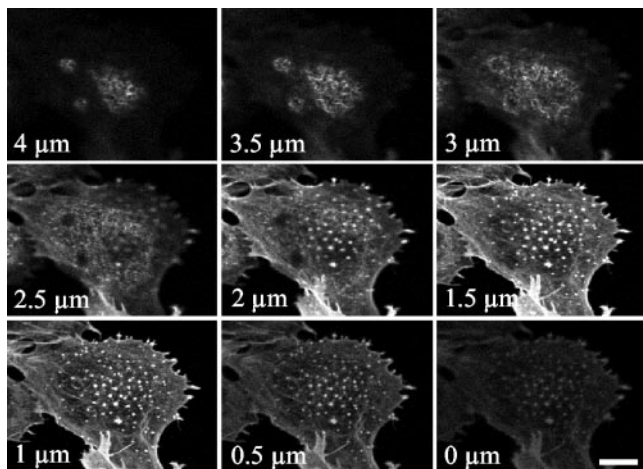


FIG. 3. Actin-rich structures are localized at the ventral surface. V12Cdc42-expressing PAE cells (24 h of induction) were fixed and stained with rhodamine-phalloidin to label F-actin. Optical sections (0.5  $\mu\text{m}$ ) are taken from the bottom to the top of the cell by confocal microscopy. Bar, 25  $\mu\text{m}$ .

actin-containing dots with the substratum (51). When cells were gently streamed with a jet of buffer, cell bodies were washed away and dots remained attached to the substratum like footprints of the ventral cell membrane (data not shown). Our data are thus consistent with the definition of podosomes as adhesive structures found at the ventral membrane of the cell and directed perpendicularly from the substratum (36). Vinculin, a focal adhesion protein normally found at the end of stress fibers in PAE cells redistributed to the actin dots (Fig. 4A). In addition, vinculin-containing adhesions were present at the cell periphery but, in most cases, did not overlap with the ends of stress fibers. Compared to focal adhesions, these complexes seemed smaller and thinner and were often colocalized with F-actin, but they did not have the elongated shape of the characteristic Rho-regulated focal adhesion. These spots located at the cell periphery were reminiscent of the previously described Cdc42- or Rac-induced focal complexes (37, 42). Using higher magnification, we observed that vinculin was organized as a ring around actin dots (Fig. 4B), consistent with the podosome structure (29). Gelsolin, an actin-binding protein essential for podosome formation in osteoclasts (5), was detected in podosomes from PAE cells, and tyrosine-phosphorylated proteins also colocalized with the actin dots (Fig. 4C). VASP (vasodilator-stimulated phosphoprotein) and cortactin were also present in the structures (data not shown). Identical experiments performed on CNF1-treated cells demonstrated the same protein distribution (data not shown). In summary, vinculin, gelsolin, tyrosine-phosphorylated proteins, VASP, and cortactin can redistribute with F-actin to form podosomes in endothelial cells in the same way as they do in osteoclasts, macrophages, or Rous sarcoma virus-transformed fibroblasts. However, in contrast with macrophages, osteoclasts, or immature dendritic cells, podosomes are not constitutively found in endothelial cells but can be induced in vitro in response to sustained activation of Cdc42.

**The machinery required for actin polymerization colocalizes with podosomes.** Cdc42 is able to induce various cellular re-

sponses via WASP, the PAK family, or ACK effectors, and we used the Cdc42 effector loop mutants as tools to dissect the molecular pathways involved in podosome induction. In a constitutively active background (provided by the L61 mutation), an additional mutation in the effector loop sequence restricts the interaction with some but not all effectors. Accordingly, the L61F37A-Cdc42 mutant is deficient for Rac activation and IQGAP1 interaction, whereas the L61Y40C-Cdc42 is unable to signal PAK/p65 or WASP (23, 26). Transient transfection of GFP-L61Cdc42 induces podosomes similarly to GFP-V12Cdc42 (c.f., Fig. 5 and 2A). The L61F37A-Cdc42 mutant retained the ability to induce podosomes, whereas expression of L61Y40C-Cdc42 in PAE cells failed to do so. Activation of Rac seems intact from the morphological appearance of the transfected cell (Fig. 5). Major actin rearrangements driven by Cdc42 involve WASP and the Arp2/3 proteins in a complex localized to areas of active actin polymerization such as lamellipodia, filopodia, and pathogen-induced actin tails (16, 55). When a GFP-tagged N-WASP construct was transfected in PAE cells, the protein was found to be associated with podosomes in more than one-third of the transfected cells (35%), whereas a diffuse rhodamine-phalloidin staining suggestive of all F-actin structure disassembly was observed in the other transfected cells (Fig. 6). An N-WASP deletion mutant ( $\Delta\text{WA}$ ) which suppresses N-WASP-dependent cellular events has identified a region essential for Arp2/3-mediated rapid actin polymerization. Expression of GFP-N-WASP- $\Delta\text{WA}$  disrupted V12Cdc42-induced podosomes in PAE cells (Fig. 6). Using antibodies against the Arp3 protein, we localized the Arp2/3 complex at podosomes (Fig. 7A). It has previously been shown that N-WASP may act in a complex with WIP and that WIP plays an important role in actin-based motility of vaccinia virus and formation of filopodia (30, 33, 53). Using a GFP-tagged WIP construct, we also found colocalization of exogenous WIP with F-actin at podosomes in V12Cdc42-expressing endothelial cells (Fig. 7B). To explore the role of WIP further, a GFP-tagged WASP-binding domain of WIP was overexpressed by means of transient transfection and cells were stimulated to form podosome by inducing the expression of V12Cdc42. We found that the WASP-binding domain of WIP displayed a dominant-negative effect on Cdc42-induced podosome formation (Fig. 7B and C), suggesting that the N-WASP-WIP complex is required for podosome assembly in PAE cells. Hence, the machinery required for actin polymerization is localized at podosomes in endothelial cells, strongly suggesting that an active actin polymerization process occurs at these sites.

**Exoenzyme C3 does not prevent Cdc42-induced podosome formation or stability.** Taken together, our data thus establish that activation of Cdc42, but not RhoA, is necessary and sufficient for podosome assembly in PAE cells. However, RhoA has been shown to be critical for de novo podosome assembly and stability in osteoclasts (6). To determine whether or not RhoA contributes to V12Cdc42-induced actin reorganization in endothelial cells, we attempted to induce podosome formation in the presence of a specific inhibitor of the Rho pathway, i.e., the C3 exoenzyme from *C. botulinum*. Using a human immunodeficiency virus-TAT-mediated delivery (48), C3 exoenzyme was introduced into V12Cdc42 PAE cells, treated or not with IPTG, and polymerized actin was examined by fluorescence microscopy after rhodamine-phalloidin staining. C3

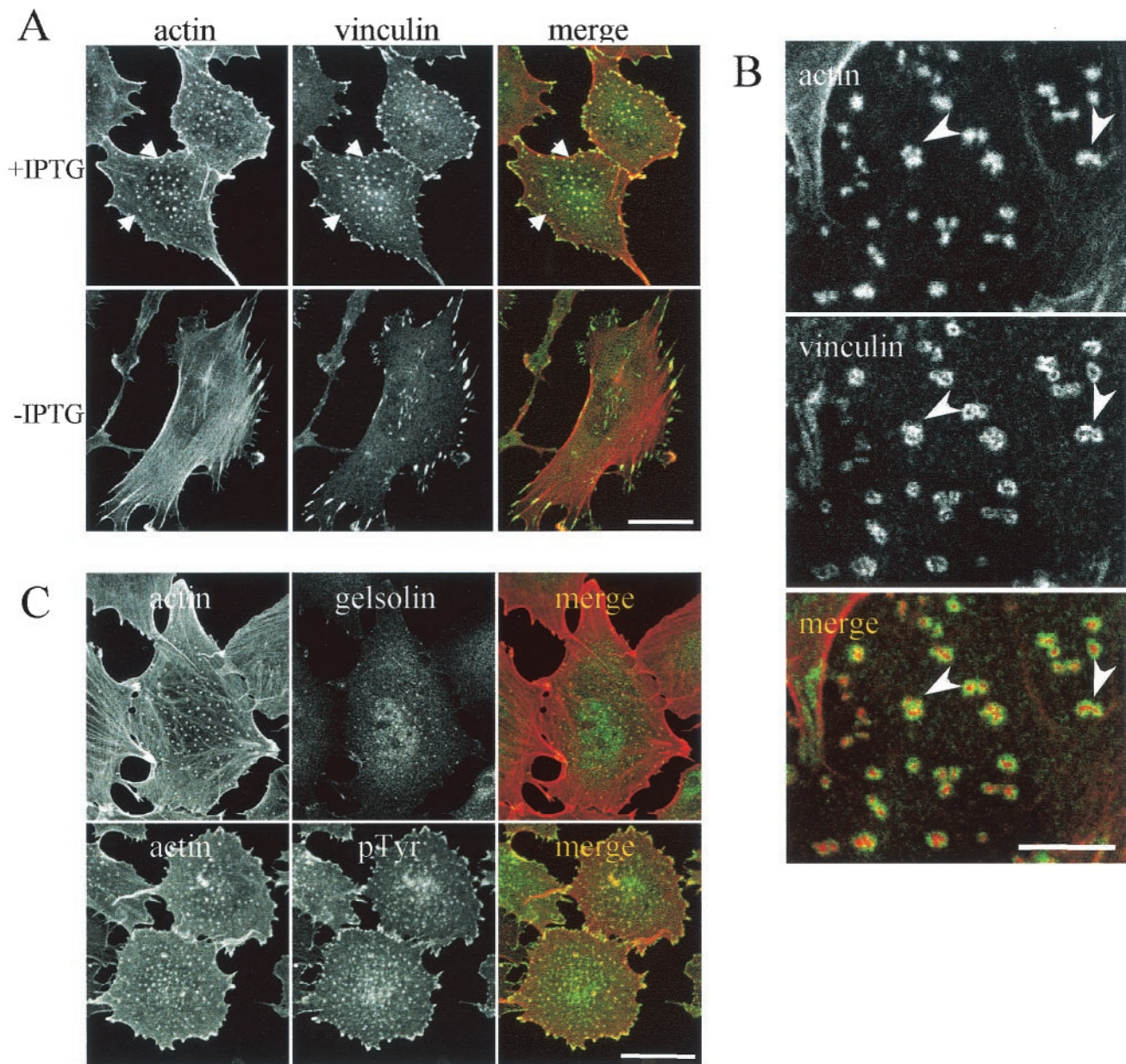


FIG. 4. Podosomal markers localized at actin-rich structures in PAE cells. (A) Vinculin localization. Established V12Cdc42 PAE cells were induced with (+IPTG) or without (–IPTG) IPTG for 24 h. Cells were fixed, permeabilized, and stained for actin (red) and vinculin (green). Bar, 50  $\mu$ m. (B) Higher magnification of a cell expressing V12Cdc42 and stained for actin (red) and vinculin (green). Note the vinculin rings and the clusters of podosomes (arrowheads). Bar, 25  $\mu$ m. (C) Gelsolin and pTyr localized to podosomes in PAE cells. PAE cells expressing V12Cdc42 (24 h of IPTG induction) were fixed with paraformaldehyde, permeabilized, and stained with gelsolin (green) or pTyr (green) antibodies together with phalloidin to label actin filaments (red). Bar, 50  $\mu$ m.

induced a strong cytopathogenic effect in noninduced PAE cells, consisting of the breakdown of stress fibers combined with dramatic morphological changes (Fig. 8A). Surprisingly, these profound morphological alterations were not observed in cells induced to express V12Cdc42, suggesting that activation of Cdc42 bypasses the cytopathogenic effect of C3. C3 treatment did not disturb podosome formation but accelerated the cell size increase (twofold) and enhanced the percentage of podosome-positive cells (Fig. 8B). Taken together, these results show that the Rho pathway is not

required for the formation of podosomes in endothelial cells and suggest that inactivation of Rho facilitates the establishment of the Cdc42-induced phenotypes. To confirm this result, we performed the reverse experiment where we overexpressed the constitutively active mutant of RhoA (V14RhoA) before treating them with CNF1. Transfection of a plasmid encoding GFP-tagged V14RhoA induced stress fiber formation in PAE cells which were not suppressed by CNF1 treatment (Fig. 8C). In addition, expression of V14RhoA, either as a GFP fusion protein or a myc-tagged

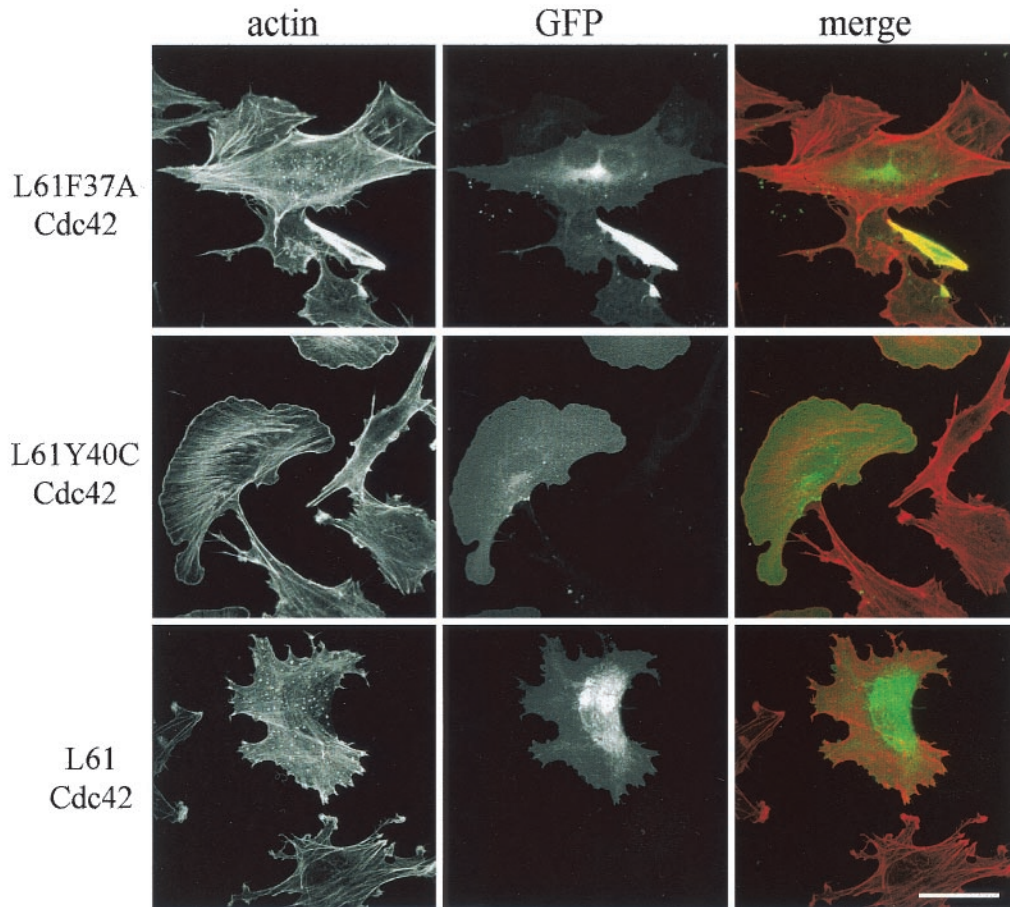


FIG. 5. L61F37ACdc42 retains the ability to induce podosomes in PAE cells. PAE cells were transfected with GFP-L61F37ACdc42, GFP-L61Y40CCdc42, or GFP-L61Cdc42. Cells were stained with rhodamine-phalloidin to visualize F-actin (red), and GFP fluorescence identifies transfected cells (green). Bar, 50  $\mu$ m.

version, strongly inhibited CNF1-induced podosome assembly (Fig. 8C and D). This result confirmed that the downregulation of RhoA activity is an important element of podosome formation in PAE cells.

**Cdc42 downregulates Rho activity.** As Rho inhibition by C3 exoenzyme facilitates the formation of podosomes, we hypothesized that Cdc42 activation could lead to the inhibition of Rho activity in PAE cells. Indeed, the disappearance of stress fibers which follows V12Cdc42 expression favors such a possibility. In PAE cells, basal Rho activity is below detection levels, so we monitored RhoA activation in response to LPA upon V12Cdc42 expression. Uninduced cells showed typical actin ruffles and stress fibers with focal adhesions as evidenced by vinculin staining (Fig. 9A). After 15 min of LPA treatment, the ruffles had disappeared and the number of stress fibers and focal adhesions had increased, consistent with Rho activity. In contrast, no morphological change was detected in LPA-treated V12Cdc42-expressing cells. The number of cells showing podosomes remained unchanged and stress fibers failed to appear, suggesting that Rho was not activated in these cells. Pull-down experiments confirmed that LPA efficiently stimulated RhoA activity in uninduced PAE cells under these conditions (Fig. 9B).

This increase in RhoA activity was completely absent in V12Cdc42-expressing cells. The linear cascade in which Cdc42 activates Rac, which in turn activates Rho as described for Swiss/3T3 cells (37), does not seem to occur in PAE cells. From these experiments, we concluded that sustained activation of Cdc42 via the expression of V12Cdc42 prevented Rho activation by LPA.

**Podosomes exist on primary endothelial cells.** Endothelial cells in the primary culture and at sustained passages retain the essential functional and biochemical characteristics typical of the endothelium (20). Endothelial cells isolated from freshly explanted human aortas and directly seeded on glass coverslips in culture medium displayed positive staining for Von Willebrand factor in Weibel-Palade bodies (Fig. 10). Double actin-vinculin staining revealed podosome-like structures and the almost complete absence of stress fibers (Fig. 10A). In addition, when cells were plated on fibronectin (Fig. 10B) or on collagen (data not shown) podosomes tended to group together in clusters. These results demonstrate that podosomes are not restricted to aortic endothelial cell lines but could also be found in primary aortic endothelial cells.

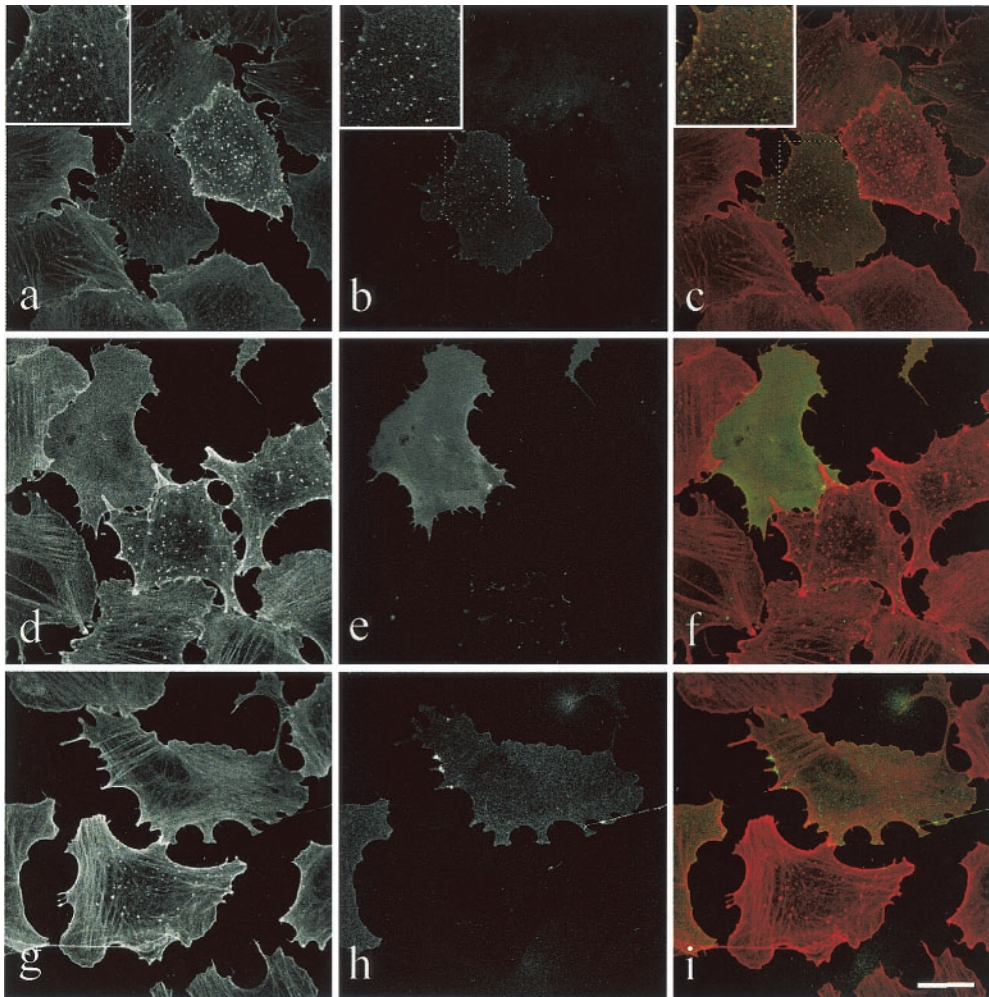


FIG. 6. N-WASP can localize at podosomes and inhibit their formation. The inducible V12Cdc42 PAE cell line was transfected with GFP-N-WASP (a to f) or GFP-N-WASP- $\Delta$ WA (g to i), and induced for 24 h with IPTG. Cells were stained with rhodamine-phalloidin to visualize F-actin (red) (a, c, d, f, g, and i), and GFP identifies transfected cells (green) (b, c, e, f, h, and i). In most cells, expression of GFP-N-WASP (d to f) and GFP-N-WASP- $\Delta$ WA (g to i) inhibits podosome formation, and N-WASP localized to podosomes (a to c) in a few cells where expression of N-WASP was low. Bar, 50  $\mu$ m.

## DISCUSSION

In the present study, we describe cytoskeletal and morphological alterations induced by sustained activation of GTPases from the Rho family in an endothelial model. Rho GTPases are targets of many bacterial toxins, including CNF1, a toxin expressed by certain uropathogenic and neonatal meningitis-inducing strains of *Escherichia coli*. Our data provide the first description of podosomes induced upon CNF1 treatment. Precise knowledge of the action of toxins is a prerequisite to understanding the pathogenesis of infectious diseases caused by toxin-producing pathogens. The discovery that CNF1-treated endothelial cells display podosomes may help in understanding the effects of toxins on bacterial invasion in vivo.

CNF1 does not induce podosome formation in other cell types. In Hep-2 cells, CNF1 induced a thickening of stress fibers and formation of membrane ruffles, the signatures of RhoA and Rac1 activities, respectively (13). On the other hand, in HeLa cells, CNF1 induced the transient formation of

microspikes and membrane ruffles (25). The effects of CNF1 appear quite different among the models used. In PAE cells, CNF1 seems to deaminate Rho, Rac, and Cdc42 to the same extent. However, GTPase degradation, which follows covalent modification (10, 22, 24), was more rapid for Rho than for Rac and Cdc42. In PAE cells, major CNF1-induced F-actin reorganization may result from the dominant contribution of Cdc42 activity to the overall cytoskeletal remodeling in this cell type. The finding that only expression of a constitutively active form of Cdc42 could mimic the effects of CNF1 on podosome induction in PAE cells is in accordance with this hypothesis. In endothelial cells isolated from human veins, CNF1 does not induce podosomes but it induces stress fibers (54), a Rho phenotype. This suggests that the effects of CNF1 in various cell types are likely dependent on the fine-tuning of the expression and spatiotemporal activation of individual Rho GTPases.

Indeed, the function of Rho GTPases in shape control, actin



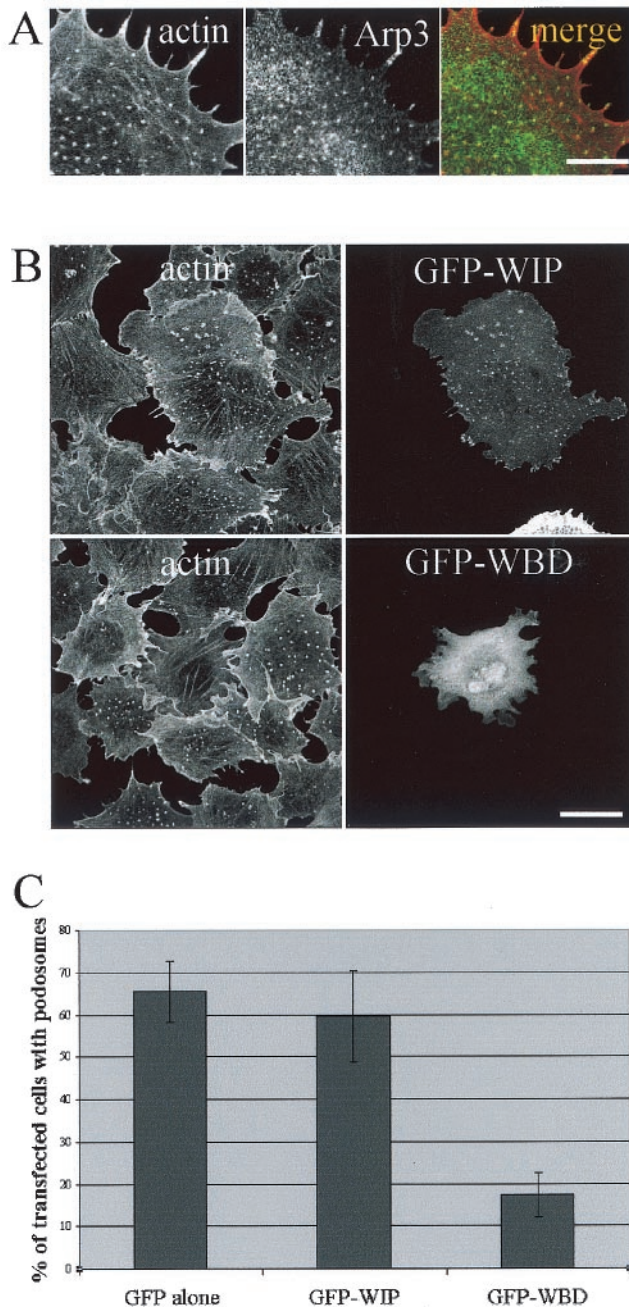


FIG. 7. Arp3 and WIP localized at podosomes in V12Cdc42-induced PAE cells. (A) Inducible V12Cdc42 PAE cells were induced for 24 h with IPTG, fixed, and processed for immunofluorescence for actin (red) and Arp3 (green) staining. Bar, 25  $\mu$ m. (B) Inducible V12Cdc42 PAE cells were transfected with either GFP-WIP or GFP-WASP binding domain (WBD) constructs and were induced for 24 h with IPTG. Cells were stained with rhodamine-phalloidin to visualize F-actin (red). Bar, 50  $\mu$ m. (C) Quantitation of the experiment described for panel B. Cells showing podosome-like structures were counted after 24 h of treatment with IPTG. Each bar represents the mean  $\pm$  standard deviation of three independent experiments.

organization, and integrin activity seems to be highly cell type dependent. Cell spreading is controlled by Cdc42 in monocytes (2), whereas it is under the control of Rac1 in T lymphocytes (11). RhoA maintains a round morphology in monocytes (1),

whereas functional RhoA is required for integrin adhesion with the extracellular matrix in fibroblasts (19). Our data indicate that the observed diversity in cytoskeletal response to individual activation of GTPases is also applicable to podosome assembly. In osteoclasts, RhoA activity is necessary and sufficient to induce de novo podosome formation, whereas activation of Cdc42 is ineffective. By contrast, in PAE cells, activation of Cdc42 is sufficient to induce podosome formation in a process independent of RhoA activity. Consistent with data obtained from dendritic immature cells (4), we found that Cdc42 plays a role in the regulation of the assembly of podosomes in endothelial cells. We also described vinculin-containing adhesion complexes at the cell periphery upon Cdc42 activation. The formation of adhesion complexes seems to be independent of Rho activity, as we demonstrated that active Cdc42 downregulates Rho activity in our model.

In response to either CNF1 or overexpression of V12Cdc42, podosome formation was associated with cell enlargement and multinucleation. Intriguingly, giant multinucleated cells seem to be somehow connected with podosome formation, since podosomes have been described in osteoclasts, foreign body giant cells (9), and differentiated trophoblast giant cells (38), which all display this phenotype at least at one point in their differentiation. However, in these cells, multinucleation results from cell fusion, whereas a defect in cytokinesis resulting in endomitosis is likely involved in CNF1-treated as well as V12Cdc42-induced PAE cells (34). Our data show that Cdc42 signaling is able to antagonize Rho activity directly at the GTPase level. A balance between GTPase activities with profound consequences on cellular morphology and behavior has been described for other models (35, 45, 57). Our data clearly show a facilitating effect of the C3-Rho inhibitory toxin on podosome formation. Rho inhibition by the C3 toxin is sufficient to induce multinucleation but not podosome assembly. These results suggest that although multinucleated cells and podosome formation are concomitantly induced in response to sustained Cdc42 activation, they appear to occur independently.

In one approach to decipher the cascade of events initiated by V12Cdc42 to stimulate podosome formation, transfection of effector loop mutants revealed that effectors of the PAK/ACK/WASP branch were involved, whereas Rac and IQGAP1 were not. WASP, and its ubiquitously expressed homolog N-WASP, are Cdc42 effectors involved in actin cytoskeleton rearrangements. In PAE cells expressing a plasmid encoding GFP-N-WASP, the protein did not aggregate around the nucleus as previously reported for WASP (50). In cells expressing a low level of plasmid, GFP-N-WASP localized to podosome structures. However, in most cells, overexpression of GFP-N-WASP led to the disassembly of podosomes and any other actin structures. In these cells, dissolution of the actin cytoskeleton is probably due to an excessive activation of N-WASP, as Cdc42 converts the dormant autoinhibited folded form of N-WASP into an active open conformation (21). Furthermore, transfection of the  $\Delta$ WA mutant form of N-WASP, which lacks a region essential to induce Arp2/3-mediated rapid actin polymerization, completely disassembled podosomes but left actin stress fibers intact. These data suggest a critical role of N-WASP in podosome formation in endothelial cells, a finding which is consistent with other models (4, 28, 32). As expected

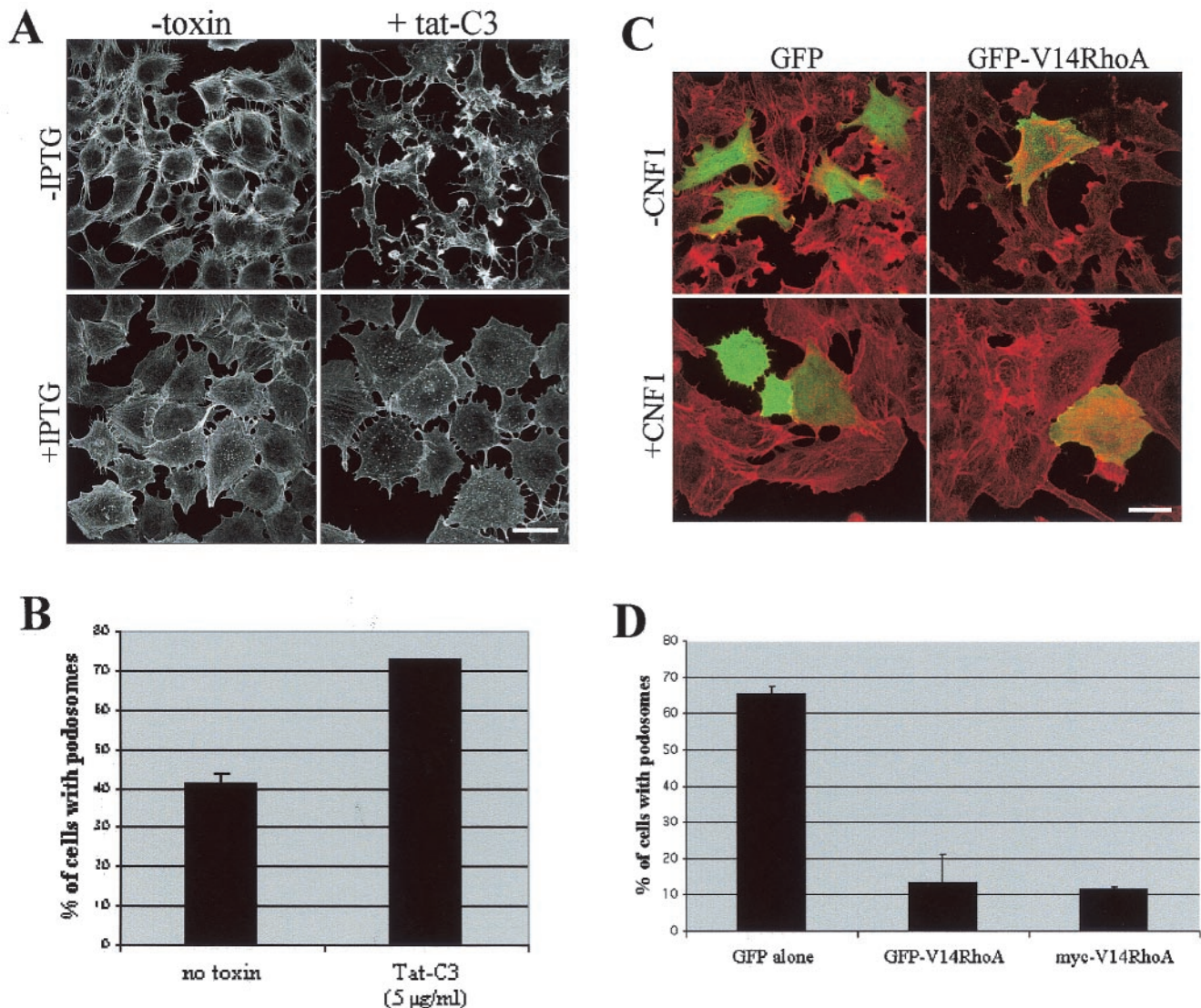


FIG. 8. Podosome formation in PAE cells is independent of Rho activity. (A) Inducible V12Cdc42 PAE cells were treated with (+tat-C3) or without (–toxin) 5 µg of Tat-C3/ml and induced for 24 h with IPTG (+IPTG) or not induced (–IPTG). F-actin was labeled with rhodamine-phalloidin. Bar, 100 µm. (B) Quantitation of the experiment described for panel A. Cells showing podosome-like structures were counted after 24 h of treatment with IPTG and toxin. Each bar represents the mean  $\pm$  standard deviation of three independent experiments. (C) PAE cells were transfected with GFP or GFP-V14RhoA constructs and treated with 0.5 µg of GST-CNF1/ml (+CNF1) for 24 h or not treated (–CNF1). Cells were then fixed, permeabilized, and stained with rhodamine-phalloidin. Bar, 100 µm. (D) Quantitation of the experiment described for panel C and of the same experiment performed with a myc-tagged version of V14RhoA. Cells showing podosome-like structures were counted after 24 h of treatment with CNF1. Each bar represents the mean  $\pm$  standard deviation of three independent experiments.

from these data, the Arp3 subunit from the Arp2/3 complex was found to be associated with the podosome structure. In addition, at the podosomes, we found WIP, a protein that binds the N-terminal region of N-WASP, with no detectable change in podosome numbers. However, overexpression of the C-terminal region of WIP, which contains the WASP-binding domain, clearly decreased Cdc42-induced podosome formation, suggesting a role for the N-WASP–WIP complex in podosome assembly in PAE cells.

Endothelial podosomes therefore appear as conical structures, randomly distributed on, but restricted to, the ventral membrane and confined to contact sites between the cell and

the substratum. The presence of endogenous tyrosine-phosphorylated proteins, together with the colocalization of proteins involved in actin polymerization and cytoskeleton organization, such as VASP, cortactin, gelsolin, talin, and Arp2/3, thereby confirm that these structures are genuine podosomes.

From a functional point of view, our data indicate that the machinery required for actin polymerization is localized at these podosomes, thus suggesting that podosomes are dynamic structures. We take this to mean either that podosomes are dedicated to a specific physiological process such as angiogenesis, vascular permeability, transcytosis, or extravasation of blood leukocytes or that they represent the manifestation of a

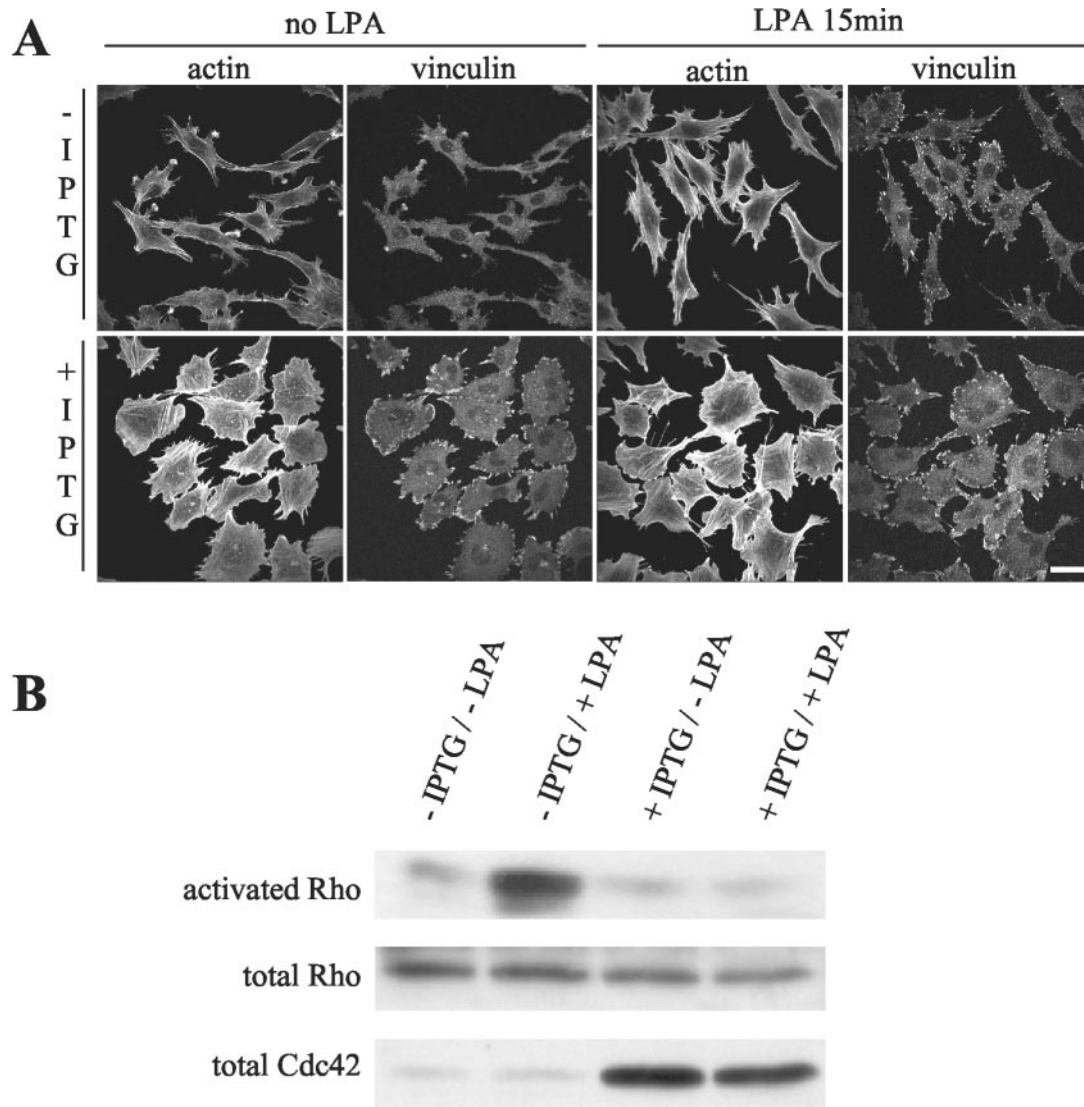


FIG. 9. V12Cdc42 downregulates Rho activity. Inducible V12Cdc42 PAE cells were serum starved and induced (+IPTG) or not (–IPTG) for 24 h with IPTG and then treated or not with 2  $\mu$ g of LPA/ml for 15 min. (A) Cells were fixed and stained for actin and vinculin. Bar, 100  $\mu$ m. (B) Cells were lysed, and GTP-bound Rho was affinity precipitated with GST-RBD-rotectin and revealed by Western blotting with anti-Rho antibody. +, present; –, absent.

pathological status, with inevitable consequences on endothelial cell functions.

PAE cells treated with CNF1 and expressing podosomes display active Cdc42 and Rac, whereas Rho is inactive. A similar pattern of Rho GTPase activities has been observed in the physiological response of human dermal microvascular endothelial cells to vascular endothelial growth factor (VEGF) (49). VEGF-treated human dermal microvascular endothelial cells displayed increased migration without podosome formation. In this model, activation of Rho decreases VEGF-stimulated motility. From this comparison, we conclude that endothelial cells from distinct vascular beds may respond differently. Alternatively, the Cdc42 effect which stimulated podosome formation in PAE cells might be outside of the physiologic VEGF response.

A unique feature of endothelial cells is that they are the

main actors of angiogenesis, a process involving interaction of endothelial cells with the extracellular matrix. The involvement of podosomes in cell adhesion is suggested by their exclusive localization at the ventral plasma membrane of the cell and confirmed by the footprints left behind when cells are gently streamed with a jet of buffer (reference 51 and this paper). In other cell types in which podosomes are found, they have been characterized as highly adhesive structures or they have been shown to be associated with a migratory behavior. In fact, the migratory or adhesive phenotype seems to be dependent on the spatial distribution of the podosomes in the cells. In osteoclasts located at the periphery, podosomes allow firm adhesion to the substratum during the process of bone resorption. When localized at the leading edge, podosomes promote cell migration (46). PAE cells harboring podosomes are nonmotile cells in the standard culture conditions described herein (V.

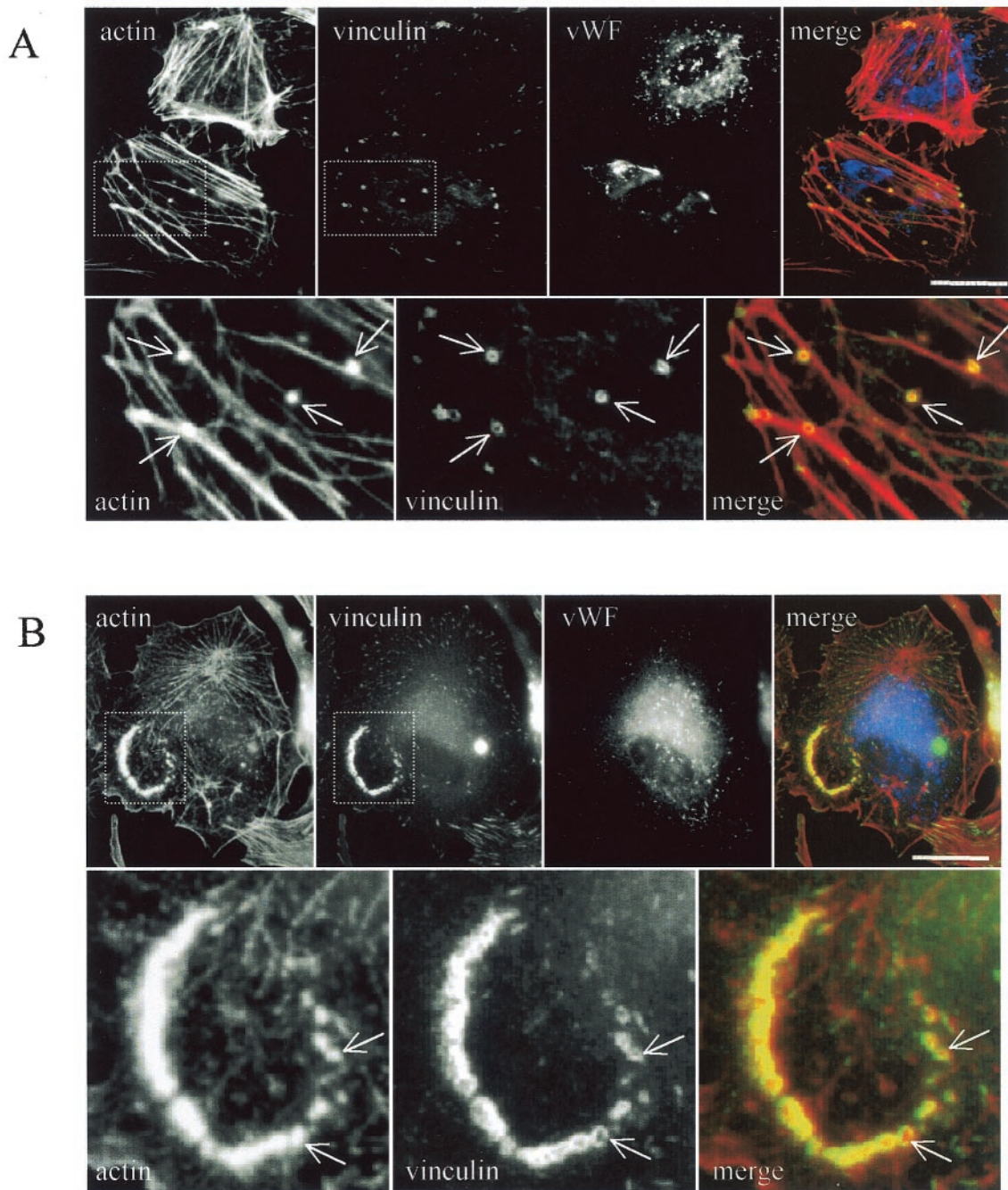


FIG. 10. Podosomes are detected on aortic endothelial cells in a primary culture. Human endothelial cells were prepared from freshly explanted aorta fragments and directly seeded on glass coverslips (A) or on fibronectin-coated coverslips (B). Cells were fixed and processed for immunofluorescence with rhodamine-phalloidin, anti-vinculin, and anti-Von-Willebrand factor antibodies (vWF). Note the presence of podosomes (arrows) visualized as actin dots surrounded by vinculin rings. Bar, 50  $\mu$ m.

Moreau and F. Tatin, unpublished data). However, explanted aortic endothelial cells revealed alteration in podosome distribution in response to either collagen or fibronectin. Detailed analysis of podosome distribution under different experimental conditions will help to determine whether cell behavior can be shifted towards a migratory phenotype in other experimental settings.

Besides adhesion, other directions of investigation include

invasiveness, trafficking, and transcytosis. The ability of podosomes harboring cells to move across anatomical boundaries has been linked to the presence of matrix metalloproteases in podosomes, so the enzymatic pattern of PAE cells harboring podosomes is therefore under current investigation. A role for podosomes in vesicular transport is another attractive possibility, since both the actin cytoskeleton and Cdc42 affect membrane trafficking. Cdc42 drives vesicle movement through

Arp2/3-modulating actin polymerization at the surface of the vesicle in the same way as it does at the plasma membrane.

Discovering the physiological inducers of podosomes in endothelial cells will help to determine their roles *in vivo*. In this study, podosomes were inducible by sustained activation of Cdc42 and were also found in human primary endothelial cells. But it is not yet known whether podosomes are transient F-actin structures occurring in a given step of a process or constitutively found in defined situations such as pathological settings. Podosomes assemble in osteoclasts as the cells differentiate in response to cytokines such as RANKL (39). In human blood-derived monocytes, podosomes form as cells fuse in response to interleukin-13, and in immature dendritic cells, podosomes are induced by plating cells on a fibronectin-coated surface. Regarding aortic endothelial cells, podosomes could be inducible *in vivo* in response to inflammatory such as interleukin-1 and tumor necrosis factor alpha, known to activate Cdc42 in other cell types (40). Cosignals from the extracellular matrix might also contribute to Cdc42 activation or to sustaining its activity (56). Finally, endothelial cells are exposed to hemodynamic forces in the form of shear stress and mechanical strains imposed by circulating blood. These are recognized factors involved in the control of endothelial cytoskeletal structure and function. Shear stress has been found to activate Cdc42 in endothelial cells (27) and could therefore be involved in the induction of these structures *in vivo*.

Understanding the phenotypic and functional changes brought about by the appearance of these structures will help in unraveling the functional characteristics of these cells, thereby improving our understanding of the numerous and complex endothelial functions.

#### ACKNOWLEDGMENTS

We thank J. Bertoglio, C. Chaponnier, J. Collard (Amsterdam, The Netherlands), P. Fort, J. Saklatvala (London, United Kingdom), D. Cantrell, D. Stewart (Bethesda, Md.), M. Way (London, United Kingdom), and M. Welch (Berkeley, Calif.) for providing toxins, cell lines, constructs, and antibodies. We thank Laura Spinardi (Milan, Italy) for help with gelsolin antibodies and Sandra Sena (U441) for help with manipulating explants. We thank I. Kramer and J. Bertoglio for critical reading of the manuscript.

This work was supported by grants from the Association pour la Recherche contre le Cancer (contract no. 5546) and from La Ligue Nationale contre le Cancer.

#### REFERENCES

- Aepfelbacher, M. 1995. ADP-ribosylation of Rho enhances adhesion of U937 cells to fibronectin via the alpha 5 beta 1 integrin receptor. *FEBS Lett.* **363**:78–80.
- Aepfelbacher, M., F. Vauti, P. C. Weber, and J. A. Glomset. 1994. Spreading of differentiating human monocytes is associated with a major increase in membrane-bound CDC42. *Proc. Natl. Acad. Sci. USA* **91**:4263–4267.
- Antonov, A. S., M. A. Nikolaeva, T. S. Klueva, A. Romanov Yu, V. R. Babaev, V. B. Bystrevskaya, N. A. Perov, V. S. Repin, and V. N. Smirnov. 1986. Primary culture of endothelial cells from atherosclerotic human aorta. Part 1. Identification, morphological and ultrastructural characteristics of two endothelial cell subpopulations. *Atherosclerosis* **59**:1–19.
- Burns, S., A. J. Thrasher, M. P. Blundell, L. Machesky, and G. E. Jones. 2001. Configuration of human dendritic cell cytoskeleton by Rho GTPases, the WAS protein, and differentiation. *Blood* **98**:1142–1149.
- Chellaiyah, M., N. Kizer, M. Silva, U. Alvarez, D. Kwiatkowski, and K. A. Hruska. 2000. Gelsolin deficiency blocks podosome assembly and produces increased bone mass and strength. *J. Cell Biol.* **148**:665–678.
- Chellaiyah, M. A., N. Soga, S. Swanson, S. McAllister, U. Alvarez, D. Wang, S. F. Dowdy, and K. A. Hruska. 2000. Rho-A is critical for osteoclast podosome organization, motility, and bone resorption. *J. Biol. Chem.* **275**:11993–12002.
- Chen, W. T. 1989. Proteolytic activity of specialized surface protrusions formed at rosette contact sites of transformed cells. *J. Exp. Zool.* **251**:167–185.
- Davis, W., L. R. Stephens, P. T. Hawkins, and J. Saklatvala. 1999. Synergistic activation of JNK/SAPK by interleukin-1 and platelet-derived growth factor is independent of Rac and Cdc42. *Biochem. J.* **338**:387–392.
- DeFife, K. M., C. R. Jenney, E. Colton, and J. M. Anderson. 1999. Cytoskeletal and adhesive structural polarizations accompany IL-13-induced human macrophage fusion. *J. Histochem. Cytochem.* **47**:65–74.
- Doye, A., A. Mettouchi, G. Bossis, R. Clement, C. Buisson-Touati, G. Flatau, L. Gagnoux, M. Piechaczyk, P. Boquet, and E. Lemichez. 2002. CNF1 exploits the ubiquitin-proteasome machinery to restrict Rho GTPase activation for bacterial host cell invasion. *Cell* **111**:553–564.
- D'Souza-Schorey, C., B. Boettner, and L. Van Aelst. 1998. Rac regulates integrin-mediated spreading and increased adhesion of T lymphocytes. *Mol. Cell. Biol.* **18**:3936–3946.
- Erickson, J. W., and R. A. Cerione. 2001. Multiple roles for Cdc42 in cell regulation. *Curr. Opin. Cell Biol.* **13**:153–157.
- Fiorentini, C., G. Donelli, P. Matarrese, A. Fabbri, S. Paradisi, and P. Boquet. 1995. *Escherichia coli* cytotoxic necrotizing factor 1: evidence for induction of actin assembly by constitutive activation of the p21 Rho GTPase. *Infect. Immun.* **63**:3936–3944.
- Flatau, G., E. Lemichez, M. Gauthier, P. Chardin, S. Paris, C. Fiorentini, and P. Boquet. 1997. Toxin-induced activation of the G protein p21 Rho by deamidation of glutamine. *Nature* **387**:729–733.
- Franke, B., J. W. Akkerman, and J. L. Bos. 1997. Rapid Ca<sup>2+</sup>-mediated activation of Rap1 in human platelets. *EMBO J.* **16**:252–259.
- Frischknecht, F., and M. Way. 2001. Surfing pathogens and the lessons learned for actin polymerization. *Trends Cell Biol.* **11**:30–38.
- Gavazzi, I., M. V. Nermut, and P. C. Marchisio. 1989. Ultrastructure and gold-immunolabelling of cell-substratum adhesions (podosomes) in RSV-transformed BHK cells. *J. Cell Sci.* **94**:85–99.
- Hawkins, P. T., A. Eguinoa, R. G. Qiu, D. Stokoe, F. T. Cooke, R. Walters, S. Wennstrom, L. Claesson-Welsh, T. Evans, M. Symons, et al. 1995. PDGF stimulates an increase in GTP-Rac via activation of phosphoinositide 3-kinase. *Curr. Biol.* **5**:393–403.
- Hotchin, N. A., and A. Hall. 1995. The assembly of integrin adhesion complexes requires both extracellular matrix and intracellular rho/rac GTPases. *J. Cell Biol.* **131**:1857–1865.
- Howard, B. V., E. J. Macarak, D. Gunson, and N. A. Kefalides. 1976. Characterization of the collagen synthesized by endothelial cells in culture. *Proc. Natl. Acad. Sci. USA* **73**:2361–2364.
- Kim, A. S., L. T. Kakalis, N. Abdul-Manan, G. A. Liu, and M. K. Rosen. 2000. Autoinhibition and activation mechanisms of the Wiskott-Aldrich syndrome protein. *Nature* **404**:151–158.
- Kovacic, H. N., K. Irani, and P. J. Goldschmidt-Clermont. 2001. Redox regulation of human Rac1 stability by the proteasome in human aortic endothelial cells. *J. Biol. Chem.* **276**:45856–45861.
- Lamarche, N., N. Tapon, L. Stowers, P. D. Burbelo, P. Aspenstrom, T. Bridges, J. Chant, and A. Hall. 1996. Rac and Cdc42 induce actin polymerization and G1 cell cycle progression independently of p65PAK and the JNK/SAPK MAP kinase cascade. *Cell* **87**:519–529.
- Lerm, M., M. Pop, G. Fritz, K. Aktories, and G. Schmidt. 2002. Proteasomal degradation of cytotoxic necrotizing factor 1-activated Rac. *Infect. Immun.* **70**:4053–4058.
- Lerm, M., J. Selzer, A. Hoffmeyer, U. R. Rapp, K. Aktories, and G. Schmidt. 1999. Deamidation of Cdc42 and Rac by *Escherichia coli* cytotoxic necrotizing factor 1: activation of c-Jun N-terminal kinase in HeLa cells. *Infect. Immun.* **67**:496–503.
- Li, R., B. Debrececi, B. Jia, Y. Goa, G. Tigyi, and Y. Zheng. 1999. Localization of the PAK1-, WASP-, and IQGAP1-specifying regions of Cdc42. *J. Biol. Chem.* **274**:29648–29654.
- Li, S., B. P. Chen, N. Azuma, Y. L. Hu, S. Z. Wu, B. E. Sumpio, J. Y. Shyy, and S. Chien. 1999. Distinct roles for the small GTPases Cdc42 and Rho in endothelial responses to shear stress. *J. Clin. Investig.* **103**:1141–1150.
- Linder, S., D. Nelson, M. Weiss, and M. Aepfelbacher. 1999. Wiskott-Aldrich syndrome protein regulates podosomes in primary human macrophages. *Proc. Natl. Acad. Sci. USA* **96**:9648–9653.
- Marchisio, P. C., M. F. Di Renzo, and P. M. Comoglio. 1984. Immunofluorescence localization of phosphotyrosine containing proteins in RSV-transformed mouse fibroblasts. *Exp. Cell Res.* **154**:112–124.
- Martinez-Quiles, N., R. Rohatgi, I. M. Anton, M. Medina, S. P. Saville, H. Miki, H. Yamaguchi, T. Takenawa, J. H. Hartwig, R. S. Geha, and N. Ramesh. 2001. WIP regulates N-WASP-mediated actin polymerization and filopodium formation. *Nat. Cell Biol.* **3**:484–491.
- Michaelson, D., J. Silletti, G. Murphy, P. D'Eustachio, M. Rush, and M. R. Philips. 2001. Differential localization of Rho GTPases in live cells: regulation by hypervariable regions and RhoGDI binding. *J. Cell Biol.* **152**:111–126.
- Mizutani, K., H. Miki, H. He, H. Maruta, and T. Takenawa. 2002. Essential role of neural Wiskott-Aldrich syndrome protein in podosome formation

- and degradation of extracellular matrix in src-transformed fibroblasts. *Cancer Res.* **62**:669–674.
33. Moreau, V., F. Frischknecht, I. Reckmann, R. Vincentelli, G. Rabut, D. Stewart, and M. Way. 2000. A complex of N-WASP and WIP integrates signalling cascades that lead to actin polymerization. *Nat. Cell Biol.* **2**:441–448.
  34. Muris, D., T. Verschoor, N. Divecha, and R. Michalides. 2002. Constitutive active GTPases Rac and Cdc42 are associated with endoreplication in PAE cells. *Eur. J. Cancer* **38**:1775.
  35. Nimmual, A. S., L. J. Taylor, and D. Bar-Sagi. 2003. Redox-dependent downregulation of Rho by Rac. *Nat. Cell Biol.* **5**:236–241.
  36. Nitsch, L., E. Gionti, R. Cancedda, and P. C. Marchisio. 1989. The podosomes of Rous sarcoma virus transformed chondrocytes show a peculiar ultrastructural organization. *Cell Biol. Int. Rep.* **13**:919–926.
  37. Nobes, C. D., and A. Hall. 1995. Rho, rac, and cdc42 GTPases regulate the assembly of multimolecular focal complexes associated with actin stress fibers, lamellipodia, and filopodia. *Cell* **81**:53–62.
  38. Parast, M. M., S. Aeder, and A. E. Sutherland. 2001. Trophoblast giant-cell differentiation involves changes in cytoskeleton and cell motility. *Dev. Biol.* **230**:43–60.
  39. Pfaff, M., and P. Jurdic. 2001. Podosomes in osteoclast-like cells: structural analysis and cooperative roles of paxillin, proline-rich tyrosine kinase 2 (Pyk2) and integrin  $\alpha$ V $\beta$ 3. *J. Cell Sci.* **114**:2775–2786.
  40. Puls, A., A. G. Eliopoulos, C. D. Nobes, T. Bridges, L. S. Young, and A. Hall. 1999. Activation of the small GTPase Cdc42 by the inflammatory cytokines TNF( $\alpha$ ) and IL-1, and by the Epstein-Barr virus transforming protein LMP1. *J. Cell Sci.* **112**:2983–2992.
  41. Ren, X. D., W. B. Kiosses, and M. A. Schwartz. 1999. Regulation of the small GTP-binding protein Rho by cell adhesion and the cytoskeleton. *EMBO J.* **18**:578–585.
  42. Rottner, K., A. Hall, and J. V. Small. 1999. Interplay between Rac and Rho in the control of substrate contact dynamics. *Curr. Biol.* **9**:640–648.
  43. Sahai, E., and C. J. Marshall. 2002. ROCK and Dia have opposing effects on adherens junctions downstream of Rho. *Nat. Cell Biol.* **4**:408–415.
  44. Sander, E., S. V. Delft, J. T. Klooster, T. Reid, R. V. D. Kammen, F. Michiels, and J. Collard. 1998. Matrix-dependent Tiam1/Rac1 signaling in epithelial cells promotes either cell-cell adhesion or cell migration and is regulated by phosphatidylinositol 3-kinase. *J. Cell Biol.* **143**:1385–1398.
  45. Sander, E. E., J. P. ten Klooster, S. van Delft, R. A. van der Kammen, and J. G. Collard. 1999. Rac downregulates Rho activity: reciprocal balance between both GTPases determines cellular morphology and migratory behavior. *J. Cell Biol.* **147**:1009–1022.
  46. Sanjay, A., A. Houghton, L. Neff, E. DiDomenico, C. Bardelay, E. Antoine, J. Levy, J. Gailit, D. Bowtell, W. C. Horne, and R. Baron. 2001. Cbl associates with Pyk2 and Src to regulate Src kinase activity,  $\alpha$ (v) $\beta$ (3) integrin-mediated signaling, cell adhesion, and osteoclast motility. *J. Cell Biol.* **152**:181–195.
  47. Schmidt, G., P. Sehr, M. Wilm, J. Selzer, M. Mann, and K. Aktories. 1997. Gln 63 of Rho is deamidated by Escherichia coli cytotoxic necrotizing factor-1. *Nature* **387**:725–729.
  48. Sebbagh, M., C. Renvoize, J. Hamelin, N. Riche, J. Bertoglio, and J. Breard. 2001. Caspase-3-mediated cleavage of ROCK I induces MLC phosphorylation and apoptotic membrane blebbing. *Nat. Cell Biol.* **3**:346–352.
  49. Soga, N., N. Namba, S. McAllister, L. Cornelius, S. L. Teitelbaum, S. F. Dowdy, J. Kawamura, and K. A. Hruska. 2001. Rho family GTPases regulate VEGF-stimulated endothelial cell motility. *Exp. Cell Res.* **269**:73–87.
  50. Symons, M., J. M. Derry, B. Karlak, S. Jiang, V. Lemahieu, F. McCormick, U. Francke, and A. Abo. 1996. Wiskott-Aldrich syndrome protein, a novel effector for the GTPase CDC42Hs, is implicated in actin polymerization. *Cell* **84**:723–734.
  51. Tarone, G., D. Cirillo, F. Giancotti, P. Comoglio, and P. Marchisio. 1985. Rous sarcoma virus-transformed fibroblasts adhere primarily at discrete protrusions of the ventral membrane called podosomes. *Exp. Cell Res.* **159**:141–157.
  52. Van Aelst, L., and C. D'Souza-Schorey. 1997. Rho GTPases and signaling networks. *Genes Dev.* **11**:2295–2322.
  53. Vetterkind, S., H. Miki, T. Takenawa, I. Klawitz, K. H. Scheidtmann, and U. Preuss. 2002. The rat homologue of Wiskott-Aldrich syndrome protein (WASP)-interacting protein (WIP) associates with actin filaments, recruits N-WASP from the nucleus, and mediates mobilization of actin from stress fibers in favor of filopodia formation. *J. Biol. Chem.* **277**:87–95.
  54. Vouret-Craviari, V., C. Bourcier, E. Boulter, and E. Van Obberghen-Schilling. 2002. Distinct signals via Rho GTPases and Src drive shape changes by thrombin and sphingosine-1-phosphate in endothelial cells. *J. Cell Sci.* **115**:2475–2484.
  55. Welch, M. D., A. Iwamatsu, and T. J. Mitchison. 1997. Actin polymerization is induced by Arp2/3 protein complex at the surface of Listeria monocytogenes. *Nature* **385**:265–269.
  56. Weston, C. A., L. Anova, C. Rialas, J. M. Prives, and B. S. Weeks. 2000. Laminin-1 activates Cdc42 in the mechanism of laminin-1-mediated neurite outgrowth. *Exp. Cell Res.* **260**:374–378.
  57. Yamaguchi, Y., H. Katoh, H. Yasui, K. Mori, and M. Negishi. 2001. RhoA inhibits the nerve growth factor-induced Rac1 activation through Rho-associated kinase-dependent pathway. *J. Biol. Chem.* **276**:18977–18983.
  58. Zhang, D., N. Udagawa, I. Nakamura, H. Murakami, S. Saito, K. Yamasaki, Y. Shibasaki, N. Morii, S. Narumiya, N. Takahashi, et al. 1995. The small GTP-binding protein, rho p21, is involved in bone resorption by regulating cytoskeletal organization in osteoclasts. *J. Cell Sci.* **108**:2285–2292.